Electrochemical Materials and Technologies

Revealing the effect of local structure on phase equilibria in binary molten salts

Mikhail Kobelev [a] [*]
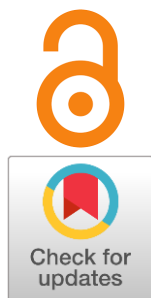
Liquidus curves for LiF-KF and LiF-KCl mixtures are calculated from the two-phase technique in the framework of molecular dynamics simulation. The calculated topology of the solid-liquid equilibria is in excellent correspondence with the experimental data. The local structures in liquid LiF-KF and LiF-KCl mixtures are analyzed by the partial structure factors (PSFs) calculations. For the reciprocal mixture LiF-KCl of equimolar composition, the appearance of a significant intensity peak in the region of small k and only a decrease in the height of the principal peaks of the PSFs for lithium-lithium, fluorine-fluorine, and lithium-fluorine pairs is observed. An intermediate range ordering appears for the Li$^+$ and F$^-$ ions, which is associated with clustering of these species and is reflected in the s-shape form for the liquidus curve for LiF-KCl mixture.

1. Introduction

Binary mixtures of alkali halides (*AHs*) with a common ion show different phase equilibria features. Melts of *AX-BX* or *AX-AY* type (here, *A* and *B* are alkali cations; *X* and *Y* are halide ions) exhibit the phase diagram patterns depending on the ionic radii ratio [1–4]. For example, binary mixtures with a common anion with the cations of close radii represent a phase diagram with a continuous series of solutions in both the solid and liquid phases. With increasing size differences between cations, simple eutectic phase diagrams are observed. Such a type is made up of mixtures of Na*X*-Rb*X*, Na*X*-Cs*X*, Li*X*-K*X*, and some others. When size differences reach the maximum possible values, experiments show the presence of certain compounds in the crystal structure, which differs significantly from the rock salt lattice. For example, in the case of Li*X*-Rb*X* and Li*X*-Cs*X* mixtures, these are LiRb*X*$_2$ and LiCs*X*$_2$ [5–8].

In the liquid region of the phase diagram, binary mixtures of *AHs* with common ions do not have any observable features. The situation changes if one considers mixtures of *AHs* consisting of four different ions, i.e., *AX-BY* type mixtures. Beyond the features mentioned above, the diagrams exhibit an immiscibility gap in the liquid phase region for this type of system [9–11]. In this case, as was shown in [12], the key parameter controlling the phase equilibrium is the difference in the radii of the mixture components *AX* and *BY*. Due to the particularity of the Coulomb interaction, the screening ability of ions of different sizes becomes the main driver. A general pattern for segregation is that a smaller cation tends to surround itself with a smaller anion and vice versa. As a result, the system splits into two liquid phases; in a macroscopic sense, it is a solution for one component in another. Experiments show that liquid-phase immiscibility is observed only if 1) one of the components is lithium fluoride and 2) the size difference between the mixture's components becomes more significant than a specific value [9]. For example, for the binary mixture of LiF-KBr, the phase diagram has an immiscibility gap, whereas the

a: Institute of High-Temperature Electrochemistry, Ural Branch of RAS, Ekaterinburg 620009, Russia

* Corresponding author: m.kobelev@ihte.ru

LiF-KCl mixture exhibits a simple eutectic-type diagram [13].

The appearance of an immiscibility gap for some mixtures that consist of components of identical chemical nature with the same type of interparticle interaction is due to the complication of the local structure. It should be noted that *AHs* are characterized by ionic chemical bonds with the formal charge of ions of ± 1.

The microscopic structure and most of the physicochemical properties of pure alkali halides are accurately described within a simple model of charged hard spheres [14–16] and the rigid ion model (RIM) [17–19]. Therefore, rigorous models considering the Coulomb nature of interactions are suitable for the theoretical study of the intermediate range ordering in binary mixtures of alkali halides.

In the pioneering study by Ribeiro [20], the structure characteristics were calculated for LiF-KF and LiCl-KCl binary mixtures. The partial structure factors (PSFs) were obtained for the equimolar mixture. The author used the classical molecular dynamics method and the Born-Huggins-Mayer pair potential with Fumi-Tosi parameters (BHMFT). For both considered mixtures, the Li-Li structure factor has a so-called pre-peak (or first sharp diffraction peak – FSDP) in the region of wave vector values smaller than the principal peak. For example, for the LiF-KF mixture, the position of the pre-peak for the Li-Li pair is 1.1 Å^{-1}, while the position of the principal peak is 2.5 Å^{-1}. All other partial structure factors demonstrate a standard form with the presence of a principal peak and damped oscillations. At the same time, the height of the PSF principal peak for all pairs of binary mixtures decreases compared to those for the individual salts. Also, the pre-peak height for the fluoride mixture is higher than that for the chloride mixture.

Madden and co-workers [21] simulated a series of binary mixtures: 0.25 LiF-0.75 KF, 0.5 LiF-0.5 KF, 0.75 LiF-0.25 KF, 0.25 LiF-0.75 NaF, and 0.59 LiCl-0.41 KCl. The calculations were performed using the polarized ion model (PIM) model in the temperature range of 773–1300 K. It was shown that the pre-peak at Li-Li PSFs in a long-wavelength region is preserved for all studied binary mixtures with a common anion. At the same time, it was noted that the Li-Li radial distribution functions do not exhibit unusual features except for a significant increase in the height of the principal peak. The authors concluded that the intermediate chemical ordering of lithium cations is a common property of binary mixtures of lithium halides with other *AHs*. There is a deterioration in miscibility at the microscopic level, which is a consequence of the different screening abilities of ions of different radii.

The LiF-KCl mixture is poorly described in the literature. There is a single theoretical study [22] that presents the results of molecular dynamics calculations of radial distribution functions and self-diffusion coefficients for a LiF-KCl equimolar mixture at $T = 1200$ K. An ensemble consisting of 216 ions was simulated using the BHMFT pair potential. Data on the radial distribution functions (RDFs) obtained for the binary mixture were compared with the RDFs of the pure components. Based on the changes in the height and position of the principal peaks on the partial RDFs, a generally correct conclusion was made on the tendency to form clusters consisting of Li$^+$ and F$^-$ ions due to the stronger Li$^+$-F$^-$ interaction.

Since the local structure of the melt significantly affects the patterns of phase equilibrium of AHs binary mixtures, it is relevant to perform a theoretical analysis of the observed phenomena within the framework of the same methodology. Moreover, the molecular dynamics method allows the calculation of liquidus temperatures for phase diagrams of the simple eutectic type without involving experimental data [23–25].

Two binary mixtures were chosen as objects of this theoretical study: a fluoride mixture with a common anion LiF-KF and a reciprocal mixture LiF-KCl, both with the phase diagram of a simple eutectic type. However, in the latter case, the eutectic point is strongly shifted toward KCl, and the liquidus line separating the two-phase region (LiF(solid) + melt) from the melt has an *s*-shaped form [26, 27]. This study uses the molecular dynamics method to calculate the liquidus curves and structure properties of the LiF-KF and LiF-KCl binary mixtures. An analysis of the structure features connected with the replacement of the anion in the second salt will be presented as well as the correlation of the local structure and the phase behavior of these binary mixtures. The results obtained for the phase diagrams and structure characteristics will be compared with experimental and calculated data in the literature.

2. Simulation details

The calculation of phase equilibria involves modeling large two-phase molecular dynamics cells during long simulation runs; therefore, the Born-Mayer pair potential was used. Previously, this potential, combined with the *ab initio*-based parameters, was applied to calculate the melting temperatures of *AHs* with relatively low errors [28]. The potential energy function consists of two contributions: the first is the Coulomb term; the second term describes the short-range repulsion of electron shells in exponential form (Born-Mayer):

$$U_{ij}(r) = \frac{Z_i Z_j e^2}{\varepsilon \cdot r} + A \cdot exp\left[-\frac{r}{\rho}\right], \qquad \textbf{(1)}$$

there Z_i, Z_j are the charges of interacting particles located at a distance r, ε is the dielectric constant (equal to 1 in our case), e is an electron charge. The parameters A and ρ specify the Born-Mayer repulsion were calculated in [28]. The calculation of partial structure factors $S_{\alpha\beta}(k)$ was carried out by the direct method, using particle trajectories, through the expression:

$$S_{\alpha\beta}(k) = \frac{1}{\sqrt{N_\alpha N_\beta}} \langle \sum_\alpha \sum_\beta e^{-i k \cdot (r_\alpha - r_\beta)} \rangle, \qquad \textbf{(2)}$$

here N_α is the number of particles of type α, $\boldsymbol{r}_\alpha$ is the radius vector of a particle of type α, the wave vector $\boldsymbol{k}$ is determined on an interval depending on the size of the simulated cell and its minimum value is $\boldsymbol{k} = \frac{2\pi}{L}\{1,0,0\}$. The exponent in Equation 2 in the case of homogeneous and isotropic liquids can be represented through scalar quantities describing the absolute value of the distance between particles and the value of the wave vector: $\sin(kr)/kr$. The parameter L is the length of the simulated cubic cell. In angle brackets, the summation is carried out over all particles' coordinates and averaged over the ensemble and the simulation time.

To analyze the local structure of LiF-KF and LiF-KCl binary mixtures, the equimolar compositions were simulated in the molten state at a temperature of $T = 1030$ K and standard pressure. The individual components of the mixtures (LiF, KF, and KCl) were simulated under the same conditions. LiCl melt was also simulated to compare its Li-Cl PSFs with one of the reciprocal LiF-KCl mixture. The molecular dynamic trajectories required for calculating the PSFs were obtained by simulating cubic cells containing 20000 ions for binary mixtures and 13824 for individual melts. Periodic boundary conditions were imposed. The total simulation time was 1.0 ns, with a step size of $\Delta t = 1$ fs.

The liquidus temperatures were calculated using the two-phase method described in [23]. The simulated cells are rectangular parallelepipeds with the dimensions of 40 Å × 40 Å × L_z, where the lattice parameter along the z coordinate takes the values $L_z = 85$ Å ÷ 220 Å, depending on the concentration of the binary mixture components. The core of the method is gradually heating until the cell becomes completely single-phase. The algorithm consists of sequential simulations of heating and constant-temperature conditions. The temperature at which the solid phase completely melts is the liquidus temperature for a given concentration. For the heating stages of the simulation, the heating rate of 2 K/ns was

chosen based on a reasonable balance between the accuracy of the calculated phase transition temperature and the simulation time. The error in determining liquidus temperatures by this method is about $\Delta T = \pm 30$ K.

The simulation time step for all mixtures was $\Delta t = 1$ fs. The total simulation time for each composition depended on the initial temperature at which the configuration and equilibration of the two-phase cell were performed. For the LiF-KF mixtures close to the eutectic composition, the total simulation time was about 10.0 ns. In contrast, the simulation time was 25–35 ns for the compositions far from the eutectic point. The same order of magnitude for the total simulation time, depending on the concentration of the components, was necessary for the reciprocal LiF-KCl mixture. Temperature and pressure were controlled using a thermostat and a Nose-Hoover barostat [29]. The damping parameters for temperature and pressure were 0.1 and 0.5 ps respectively. All calculations were performed in the LAMMPS package [30] using the computing resources of the Uran supercomputer at the IMM UB RAS.

3. Results and discussion

Static structure factor $S_{\alpha\beta}(k)$ reflects density fluctuations and, therefore, serves as a convenient function for describing the structure of a liquid [31]. Typical ionic melts are characterized by one principal peak at distances of the order of $k_{max} \sim \frac{2\pi}{\sigma}$, where σ is the closest distance between ions. If, for various reasons, stable density fluctuations or microheterogeneity arise in the melt volume at distances significantly greater than σ, this leads to the appearance of an additional peak in $S_{\alpha\beta}(k)$. As the fluctuations increase, the additional peak becomes more pronounced and shifts toward the region of small k. High and rapidly increasing peaks at $k \to 0$ indicate density fluctuations on the scale of the entire system, i.e., macroscopic instability.

Figure 1 shows the calculated PSFs for the potassium-potassium pair in equimolar LiF-KF and LiF-KCl mixtures, as well as for KF and KCl melts at $T = 1030$ K. When the binary mixture is formed, the intensity of the principal peak decreases as expected, and its position shifts slightly toward a larger k. This behavior of $S_{KK}(k)$ is observed for both mixtures. It is due to the number of potassium-potassium pairs per unit volume of the melt alongside a slight decrease in the distance between the cations. The $S_{KK}(k)$ graphs do not show any features indicating the formation of clusters or any segregation involving potassium cations. This is confirmed by the data in Figure 2, which shows the instantaneous configuration of

potassium cations in an equimolar LiF-KCl binary mixture. Snapshots taken at equilibrium molten state at $T = 1030$ K and every 5000 timesteps were analyzed. One of them, which corresponds to 0.5 ns, is presented in Figure 2. All other types of ions constituting the reciprocal mixture have been removed from the cell for clarity. Figure 2 shows a uniform distribution of potassium cations throughout the simulated cell.

Let us now consider the behavior of the PSFs for lithium and fluorine ions. Figure 3a shows the calculated $S_{LiLi}(k)$ for LiF-KF and LiF-KCl equimolar mixtures and the LiF melt at a temperature of $T = 1030$ K. The results of our MD calculation of $S_{LiLi}(k)$ for the binary mixture of LiF-KF agree with the data of [20] and demonstrate the presence of a small pre-peak at $k \sim 1.15$ Å^{-1}. Similarly, the $S_{FF}(k)$ calculated for LiF-KF (see Figure 3b) shows only a decrease in the principal peak alongside its slight shift toward smaller k, which also concurs with the data obtained using the BHMFT pair potential [20]. The results of the calculation of the PSFs for the binary mixture

LiF-KCl of equimolar composition are more intriguing. In this case, the PSFs calculated for lithium and fluorine ions significantly increase from approximately $k \sim 1.5$ Å^{-1} to the boundary values k_{min}. The latter are determined by the linear dimensions of the simulated cells and, in our case, are equal to 0.25 Å^{-1}. The inability to determine the position of the maxima for $S_{LiLi}(k)$ and $S_{FF}(k)$ indicates that the inhomogeneities formed with lithium and fluorine ions exceed the dimensions of the simulated cells of the LiF-KCl binary mixture. Figure 4 shows the instantaneous configuration of lithium cations in the reciprocal mixture, with other types of ions removed from the cell. This snapshot was taken under the same conditions as in Figure 2. The distribution of lithium cations in the MD cell is non-uniform. However, the scale of lithium density fluctuations in the reciprocal mixture at the studied temperature is not macroscopic. Otherwise, the simulated melt would represent two immiscible liquids separated by a surface, i.e., two separate liquid phases.
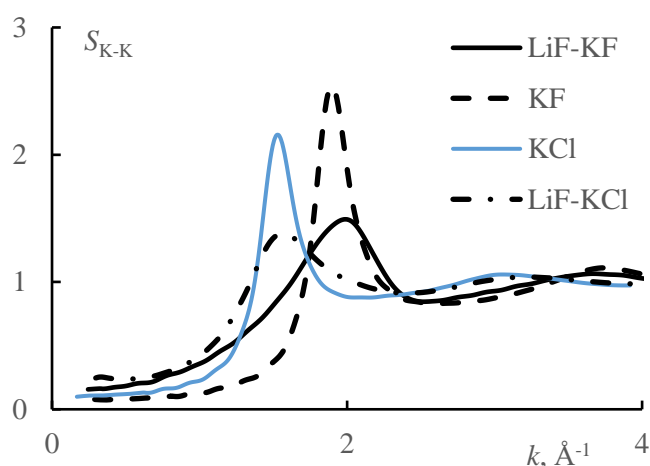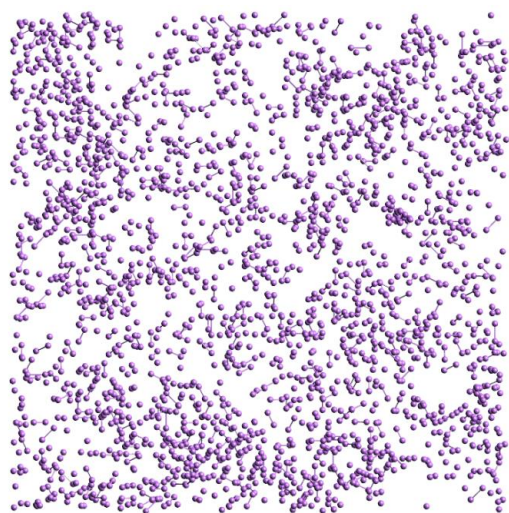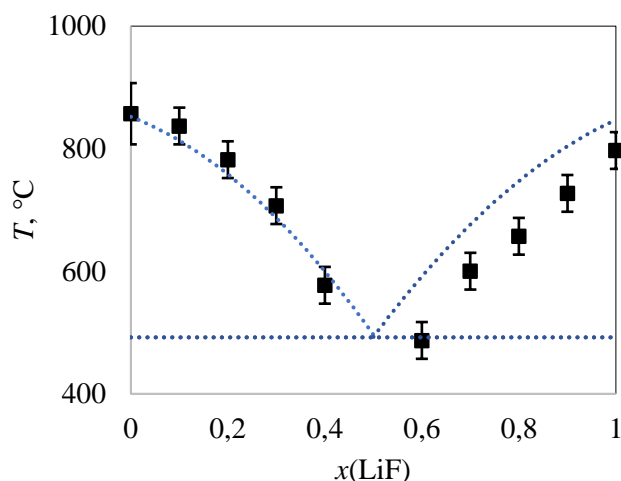

Figure 1 Structure factors $S_{KK}(k)$.
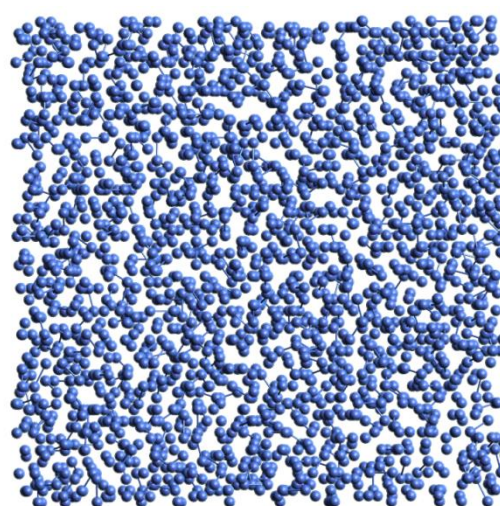
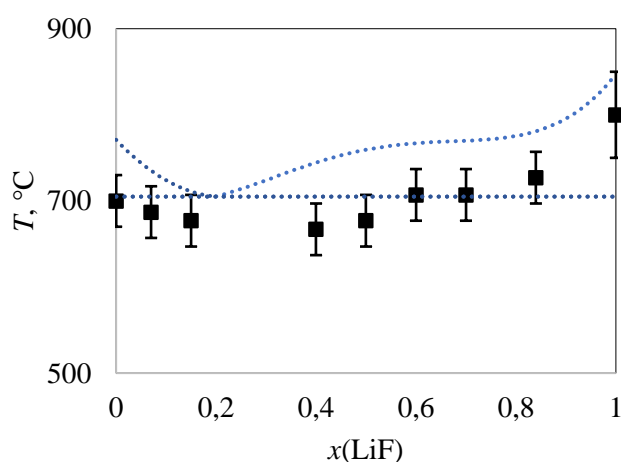**Figure 2** Snapshot of K$^+$ in LiF-KCl equimolar mixture.
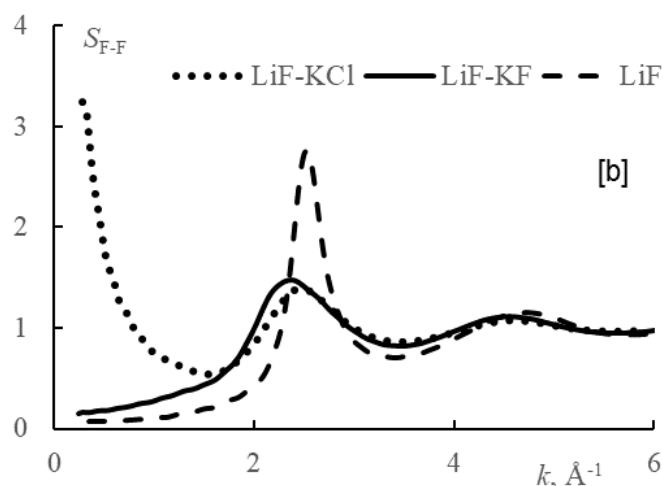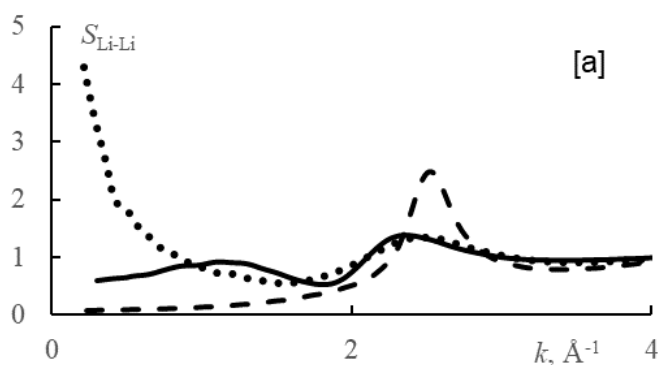
Figure 3 Calculated PSFs (a) $S_{LiLi}(k)$ and (b) $S_{FF}(k)$ for equimolar mixtures and LiF.

Figure 4 Snapshot of Li⁺ in LiF-KCl equimolar mixture.

Figure 5 (■) Liquidus curve for the LiF-KF binary mixture and their error bars for all considered compositions calculated by MD. The dashed curve denotes experimental data [32].


Figure 6 (■) Liquidus curve for the LiF-KCl binary mixture and their error bars for all considered compositions calculated by MD. The dashed curve denotes experimental data.

Let us now analyze the relationship between the described features of the local environment and phase equilibria in the studied mixtures. Lithium cations in the LiF-KF binary mixture tend to form clusters in a matrix consisting of uniformly distributed potassium cations. Such microheterogeneities have virtually no effect on the phase behavior. Figure 5 shows the calculated liquidus line for the LiF-KF binary mixture compared to the experimental data. A standard fusibility curve is observed, with an almost equimolar composition of the eutectic point.

Figure 6 presents the results of the liquidus curve calculation for the reciprocal mixture LiF-KCl compared to the experimental data [27]. Note that the data obtained by the two-phase modeling method qualitatively match the topology of the experimental curve. Assessing the quantitative agreement with the experiment, there is an acceptable error level in determining the liquidus temperatures.

The main feature of the phase diagram of the reciprocal mixture LiF-KCl is as follows: on the liquidus line, which separates the two-phase region of LiF(solid) – melt coexistence and the homogeneous melt, there is a clearly expressed inflection point. Such a shape of the coexistence curve can stem from two reasons. The first reason is the presence of a chemical compound in the region of compositions close to the inflection point, that is, in the region of the equimolar ratio of LiF and KCl. So far, there is no experimental evidence of the presence of such a compound in the system under consideration. In contrast, stable compounds have been proven experimentally for LiX-RbX, LiX-CsX (X = F, Cl, Br, I) mixtures [5]. The second explanation for such a shape of the coexistence curve is associated with an immiscibility gap, which turns out to be unstable concerning the liquidus curve. In other words, the region of limited solubility occurs at a lower temperature than the liquidus curve.

The results of the calculation of the PSF indicate the formation of large-scale, but not macroscopic, fluctuations in the density of lithium fluoride in the LiF-KCl binary mixture at temperatures above the liquidus curve. In this case, the second component of the reciprocal mixture at this temperature and concentration is uniformly distributed over the entire cell volume. It stabilizes the entire melt phase, preventing decomposition into two liquids. Figure 7 shows the calculated structure factors $S_{ClCl}(k)$ and $S_{KCl}(k)$ compared to ones for the KCl melt. It is evident that the curves do not have any pre-peaks in the region of small k, and only a decrease in the height of the principal peaks occurs.
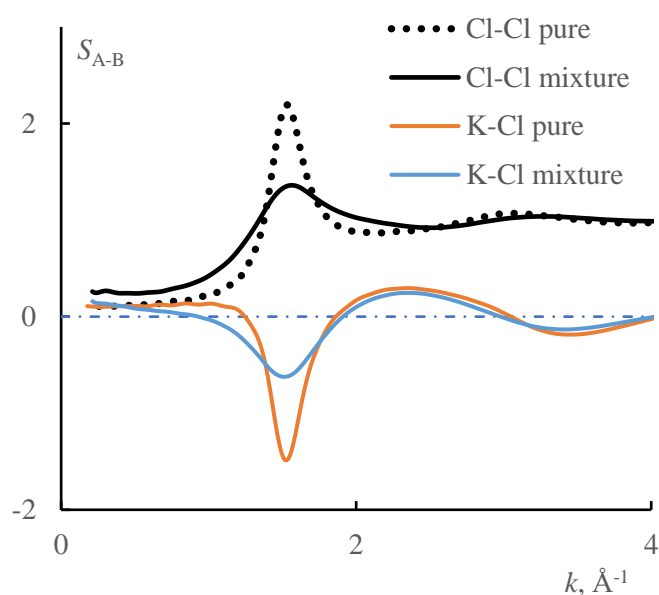
Figure 7 The structure factors $S_{ClCl}(k)$ and $S_{KCl}(k)$.

The LiF-KCl reciprocal mixture represents an example of a situation where thermal motion, which tends to mix all components, dominates the competing Coulomb interaction in the liquid phase region. The decomposition occurs during the crystallization of LiF-KCl since a eutectic mixture of components is formed. The situation changes significantly when chlorine is replaced by bromine in the second component of the mixture, i.e., if one considers the reciprocal mixture of LiF-KBr. In this case, an immiscibility gap is already formed in the liquid phase region, since the Coulomb interaction dominates thermal motion. Although the consideration of monotectic equilibrium is beyond the scope of this study, it is a promising line of research within the framework of the same theoretical approach.

Thus, the relationship between the observed phase equilibria and the local structure features is presented through the molecular dynamics modeling of binary mixtures LiF-KF and LiF-KCl. Both binary mixtures under consideration crystallize according to the eutectic equilibrium type, i.e., they demonstrate complete mixing in the liquid phase region and decomposition into components in the solid state. One of the reasons for such phase behavior is the discovered features of the local structure in the form of pre-peaks on the PSF of the lithium-lithium pair for both mixtures. Moreover, in the reciprocal LiF-KCl mixture, such pre-peak is also observed for $S_{FF}(k)$, but on an even larger scale. This leads to the appearance of an inflection point on the calculated liquidus line, which is also observed on the experimental phase diagram.

One key feature of the approach to analyzing phase equilibria presented in this paper is that no fitting empirical data were used in the calculation. All structural characteristics and temperatures of phase transitions of the binary mixtures LiF-KF and LiF-KCl are obtained within the framework of a single classical molecular dynamics method. This is a great advantage and delivers vast possibilities for predicting phase diagrams.

Supplementary materials

No supplementary materials are available.

Funding

Author contributions

Mikhail Kobelev: Writing – Review & Editing; Writing – Original draft; Visualization; Validation; Formal analysis; Data curation; Conceptualization.

Conflict of interest

The author declares that he has no known competing financial interests or personal relationships that could have appeared to influence the work reported in this paper.

Additional information

Mikhail Kobelev, Author ID: 6603014470; Web of Science ResearcherID: J-3455-2018.

References

1. Galwey AK, A view and a review of the melting of alkali metal halide crystals. Part 2. Pattern of eutectics and solid solutions in binary common ion mixtures, J. Therm. Anal. Calorim., **82** (2005) 423–437. https://doi.org/10.1007/s10973-005-0913-1

2. Oonk HAJ, Solid-state solubility and its limits. The alkali halide case, Pure Appl. Chem., **73(5)** (2001) 807–823. https://doi.org/10.1351/pac200173050807

3. van der Kemp WJM, Blok JG, van Genderen ACG, van Ekeren PJ, et. al., Binary common-ion alkali halide mixtures; a uniform description of the liquid and solid state, Thermochim. Acta, **196(2)** (1992) 301–315. https://doi.org/10.1016/0040-6031(92)80093-C

4. Garkushin IK, Burchakov AV, Emelyanova UA, Chugunova MV, Phase complex of the quinary reciprocal system Li+, Na+, K+ || F-, Cl-, Br- and investigation of the stable tetrahedron LiF-NaF-KCl-KBr, Russ. J. Inorg. Chem., **65** (2020) 1040–1046. https://doi.org/10.1134/S0036023620070086

5. Burns JH, Busing WR, Crystal structures of rubidium lithium fluoride, RbLiF₂, and cesium lithium fluoride, CsLiF₂,

Inorg. Chem., **4(10)** (1965) 1510–1512. https://doi.org/10.1021/ic50032a041

6. Pentin IV, Schön JC, Jansen M, Ab initio prediction of the low-temperature phase diagrams in the systems CsX-LiX (X=F, Cl, Br, I), Solid State Sci., **10(6)** (2008) 804–813. https://doi.org/10.1016/j.solidstatesciences.2007.06.001

7. Lipkina K, Palinka K, Geiger E, Fitzpatrick BWN, et. al., Thermodynamic investigations of the LiF-CsF and NaF-CsF pseudo-binary systems, J. Nucl. Mater., **568** (2022) 153901. https://doi.org/10.1016/j.jnucmat.2022.153901

8. Sprouster D, Zheng G, Lee SC, Olds D, et. al., Molecular structure and phase equilibria of molten fluoride salt with and without dissolved cesium: FLiNaK-CsF (5 mol %), ACS Appl. Energy Mater., **5(7)** (2022) 8067–8074. https://doi.org/10.1021/acsaem.2c00544

9. Margheritis C, Flor G, Sinistri C, Miscibility gaps in fused salts VII. Systems of LiF with alkali halides, Z. Naturforsch. A, **28** (1973) 1329–1334. https://doi.org/10.1515/zna-1973-0813

10. Stepanov VP, Babushkina LM, Dokashenko SI, Liquid + liquid equilibrium in mixtures of lithium fluoride with potassium and rubidium halides, J. Chem. Thermodyn., **51** (2012) 12–16. https://doi.org/10.1016/j.jct.2012.02.015

11. Stepanov VP, Density of separating salt melts in the two-phase region, Russ. Metall., **2022** (2022) 830–836. https://doi.org/10.1134/S0036029522080171

12. Tkachev NK, Rukavishnikova IV, Lokett VN, Stepanov VP, Density of stratified ionic melts: Experiments and theory, Russ. J. Electrochem., **43** (2007) 955–960. https://doi.org/10.1134/S1023193507080149

13. Blander M, Topol LE, The topology of phase diagrams of reciprocal molten salt systems, Inorg. Chem., **5(10)** (1966) 1641–1645. https://doi.org/10.1021/ic50044a002

14. Xiao T, Zhou Y, Jiang H, Surface tension of simple molten salts: Insight from a charged hard sphere model, J. Phys. Chem. B, **128(32)** (2024) 7882–7887. https://doi.org/10.1021/acs.jpcb.4c03118

15. Davydov AG, Tkachev NK, Heat capacity of molten alkali halides, J. Mol. Liq., **356** (2022) 119032. https://doi.org/10.1016/j.molliq.2022.119032

16. Vega C, Bresme F, Abascal JLF, Fluid-solid equilibrium of a charged hard-sphere model, Phys. Rev. E, **54** (1996) 2746. https://doi.org/10.1103/PhysRevE.54.2746

17. Dixon M, Gillan MJ, Structure of molten alkali chlorides I. A molecular dynamics study, Phil. Mag. B, **43(6)** (1981) 1099–1112. https://doi.org/10.1080/01418638108222577

18. Adams DJ, McDonald IR, Rigid-ion models of the interionic potential in the alkali halides, J. Phys. C: Solid State Phys., **7(16)** (1974) 2761–2775. https://doi.org/10.1088/0022-3719/7/16/009

19. Wang J, Sun Z, Lu G, Yu J, Molecular dynamics simulations of the local structures and transport coefficients of molten alkali chlorides, J. Phys. Chem. B, **118(34)** (2014) 10196–10206. https://doi.org/10.1021/jp5050332

20. Ribeiro MCC, Chemla effect in molten LiCl/KCl and LiF/KF mixtures, J. Phys. Chem. B, **107(18)** (2003) 4392–4402. https://doi.org/10.1021/jp027261a

21. Salanne M, Simon C, Turq P, Madden PA, Intermediate range chemical ordering of cations in simple molten alkali halides, J. Phys.: Condens. Matter, **20** (2008) 332101. https://doi.org/10.1088/0953-8984/20/33/332101

22. Shao J, Shu G, Xu H, Chen N, Molecular dynamics calculation of molten LiF, KCl and LiF-KCl (1:1) system, Chinese Phys. Lett., **6** (1989) 448–450. https://doi.org/10.1088/0256-307X/6/10/005

23. Kobelev MA, Tatarinov AS, Zakiryanov DO, Tkachev NK, Calculation of liquidus curve in phase diagram LiCl-KCl by molecular dynamics simulation, Phase Transitions, **93(5)** (2020) 504–508. https://doi.org/10.1080/01411594.2020.1758318

24. Bin Faheem A, Lee KK, Development of a neural network potential for modeling molten LiCl/KCl salts: Bridging efficiency and accuracy, J. Phys. Chem. C, **128(5)** (2024) 2163–2178. https://doi.org/10.1021/acs.jpcc.3c07010

25. DeFever RS, Maginn EJ, Computing the liquidus of binary monatomic salt mixtures with direct simulation and alchemical free energy methods, J. Phys. Chem. A, **125(38)** (2021) 8498–8513. https://doi.org/10.1021/acs.jpca.1c06107

26. Haendler HM, Sennett PS, Wheeler CM, The system LiF-LiCl, LiF-NaCl, LiF-KCl, J. Electrochem. Soc., **106** (1959) 264–268. https://doi.org/10.1149/1.2427319

27. Chartrand P, Pelton AD, Thermodynamic evaluation and optimization of the Li, Na, K, Mg, Ca // F, Cl reciprocal system using the modified quasi-chemical model, Metall. Mater. Trans. A, **32** (2001) 1417–1430. https://doi.org/10.1007/s11661-001-0231-6

28. Zakiryanov D, Kobelev M, Tkachev N, Melting properties of alkali halides and the cation-anion size difference: A molecular dynamics study, Fluid Phase Equil., **506** (2020) 112369. https://doi.org/10.1016/j.fluid.2019.112369

29. Nosé S, Constant temperature molecular dynamics methods, Prog. Theor. Phys. Supp., **103** (1991) 1–46. https://doi.org/10.1143/PTPS.103.1

30. Thompson AP, Aktulga HM, Berger R, Bolintineanu DC, et al., LAMMPS – a flexible simulation tool for particle-based materials modeling at the atomic, meso, and continuum scales, Comp. Phys. Comm., **271** (2022) 10817. https://doi.org/10.1016/j.cpc.2021.108171

31. Revere M, Tosi MP, Structure and dynamics of molten salts, Rep. Prog. Phys., **49** (1986) 1001. https://doi.org/10.1088/0034-4885/49/9/002

32. Aukrust E, Björge B, Flood H, Førland T, Activities in molten salt mixtures of potassium-lithium-halide mixtures: A preliminary report, Ann. N.Y. Acad. Sci., **79(11)** (1960) 830–837. https://doi.org/10.1111/j.1749-6632.1960.tb42757.x